Earthquake-Induced Liquefaction Effects on a Shallow Foundation

A. S. P. S Marques & P. A. L. F. Coelho
Department of Civil Engineering, University of Coimbra, Portugal

U. Cilingir
Department of Engineering, University of Sheffield, UK

S. K. Haigh & G. Madabhushi
Department of Engineering, University of Cambridge, UK

SUMMARY:
Earthquake-induced liquefaction is a major threat, frequently resulting in the failure of critical infrastructures and causing severe disruption of social and economic activities. Dynamic centrifuge experiments were carried out as part of a Transnational Access to the experimental facilities of the Schofield Centre - Cambridge University Engineering Department -, granted through SERIES research project, focusing on the centrifuge modelling of seismic liquefaction effects and mitigation in shallow foundations. The centrifuge test described in this paper assesses the performance of a single-degree-of-freedom square footing exerting a bearing pressure of 95 *kPa* on the soil foundation. The settlements of the structure, the excess pore pressure developed in the soil foundation during the earthquake and its subsequent dissipation and the accelerations of the footing are presented, clearly showing the large effects induced by earthquake-induced liquefaction on shallow foundations.

Keywords: shallow foundation; liquefaction effects; centrifuge modelling; earthquake.

1. INTRODUCTION

Liquefaction is a phenomenon in which the strength and stiffness of a soil is reduced due to large effective stress degradation caused by earthquake shaking or other rapid loading. Liquefaction and related phenomena have been responsible for tremendous damage in historical earthquakes around the world. Even if this phenomenon has been worldwide known for centuries, it was more thoroughly brought to the engineer's attention after the 1964 Niigata and 1964 Alaska earthquakes. It was also responsible for a massive part of the destruction occurred in San Francisco's Marina District during the 1989 Loma Prieta earthquake, and in Port of Kobe during the 1995 Great Hanshin earthquake. More recently liquefaction was largely responsible for extensive damages during the 2010 Canterbury and 2011 Christchurch earthquakes.

Earthquake-induced liquefaction is most commonly observed in loose, saturated, clean sand deposits. This is because looser sand tends to compress when a load is applied, unlike denser sands which tend to dilate during shearing, at least after some strains are imposed. If the soil is fully saturated, when the soil is compressed, the water pressure tends to increase and attempts to flow out from the soil to regions with lower pore water pressure (usually upwards on the way to the ground surface). However, if the loading is rapidly applied and is large enough, or if it is repeated many times at relatively high frequencies, as in an earthquake, the nearly undrained condition may result in partial or total effective stress loss. When this phenomenon occurs, the strength and stiffness of the soil decreases and the ability of a soil deposit to support shallow foundations is dramatically reduced.

As shallow foundations are often used as footings of structures such as bridges and other constructions built on loose granular deposits, their situation is particularly critical, as they are sometimes located in saturated soils that form the ideal conditions for liquefaction to occur. Thus, it becomes essential to study how these structures perform when subjected to the phenomenon of liquefaction. In view of the limitations of full scale observations during real events, resulting from temporal and spatial unpredictability of earthquakes, and the difficulties involved with numerical modelling of these problems, due to the complex behaviour of liquefiable soil, centrifuge modelling emerges as a key tool in research. In fact, taking into account that the soil physical and stress conditions are mimicked, centrifuge modelling is able to capture the true soil behaviour under realistic loading, provided that the boundary conditions of the problem are appropriately set. The work described in this paper is based on a centrifuge test performed to evaluate the earthquake-induced liquefaction effects on a simple square shallow foundation.

2. CENTRIFUGE EXPERIMENT

Dynamic centrifuge modelling was conducted using the 10 m diameter Turner Beam Centrifuge at the Schofield Centre, University of Cambridge, which is described in detail by Schofield (1980). The actuator used in this centrifuge test is known as SAM – Stored Angular Momentum (Madabhushi et al., 2001), and is able to generate near sinusoidal horizontal acceleration inputs of chosen duration and amplitude, which are considered very valuable for fundamental research on earthquake effects. The centrifuge model was prepared inside an ESB container, which was designed to minimize detrimental boundary effects during centrifuge modelling (Schofield and Zeng, 1992).

A single centrifuge experiment was performed to gain insight into the liquefaction effects caused by an earthquake on a single square shallow foundation exerting a bearing pressure of 95 *kPa* on the underlying soil. A scheme of the model, built at a 1:50 scale since the test was carried out at a centrifuge acceleration of 50g, is presented in Figure 2.1. As the figure shows, the experiment was performed using two different structures placed in opposite sides of the model. This paper only describes the performance of the heavier structure, which is located in left side of the scheme, using the results in prototype scale except where mentioned. As shown in Figure 2.1, the centrifuge model included a liquefiable soil layer thickness (H_L) of 360 mm (representing a prototype of 18 meters deep) and it had a nominal relative density (D_r) of approximately 50%. The sand was placed in the model with the help of an automatic sand pourer, whose performance is depicted by Madabhushi et al. (2006). The sand used in the model was a fine, uniform Hostun sand, with a D_{50} of 150 μm. A solution of Hydroxypropyl Methylcellulose in water was used as the pore fluid with a viscosity of approximately 50 (±2) times that of water, in order to obtain the so-called viscosity scaling and overcome the conflict between time scale in flow and dynamic phenomena (Stewart et al., 1998). The model was placed under vacuum and de-aired fluid was slowly introduced into the sand from the bottom, using small water pressure gradients. The saturation process is controlled by a computer program, thus avoiding constant human presence during this procedure.

The model of both structures consists of single-degree-of-freedom structures and, as already stated, the structure under study was designed for a static bearing pressure of 95 *kPa*. The dimensions of the structure are represented in Table 2.1. Figure 2.2 illustrates the structure prepared for placement in the centrifuge model and testing.

Table 2.1. Dimensions of the structure with a bearing pressure of 95 *kPa*.

width (mm)	length (mm)	height (mm)
60	60	24.5

The g-level was increased in 10 g intervals, at the end of each taking readings from instruments. One shaking event was applied to the base of the model of selected amplitude and frequency which was fired at 50-g level centrifuge acceleration. The earthquake fired had a 50 *Hz* frequency and lasted for 0.5 seconds, in order to simulate a real event lasting 25 seconds and having a predominant frequency of 1 *Hz*. Shaking was applied parallel to the long side of the model and the peak accelerations measured ranged between +0.324g and -0.302g in prototype scale.

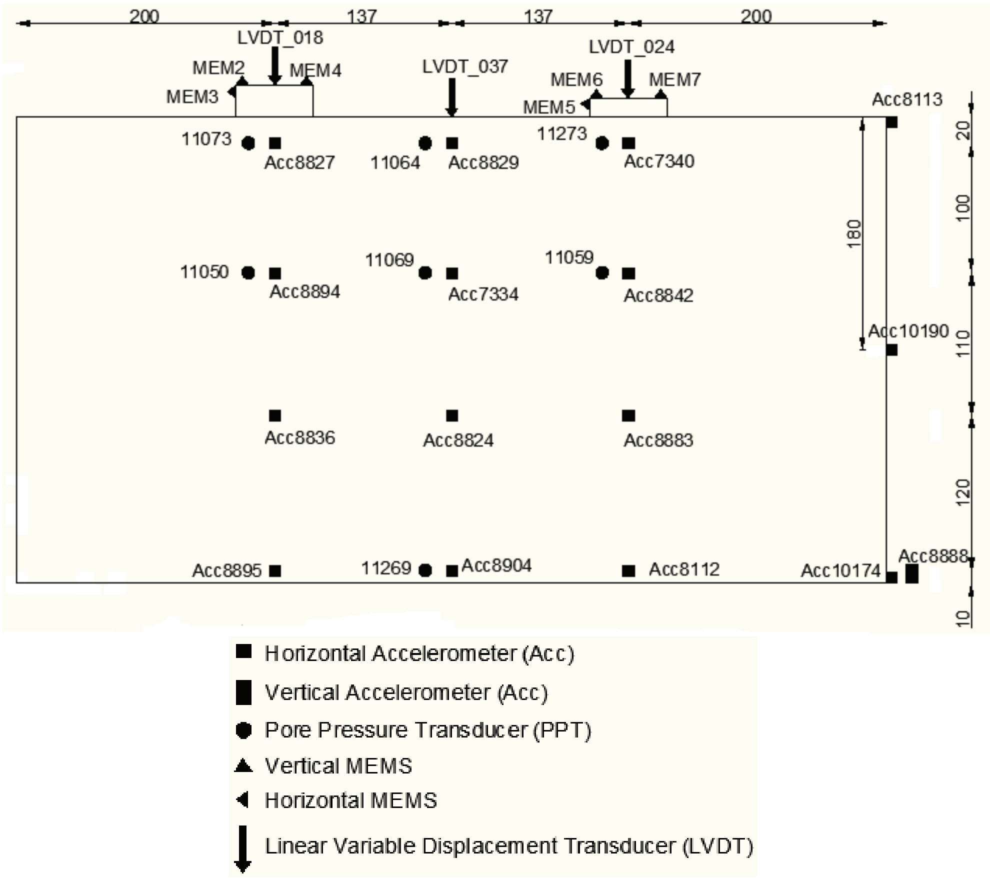

Figure 2.1. Centrifuge Model Layout (Cross Section View, model dimensions) – all units are in mm.

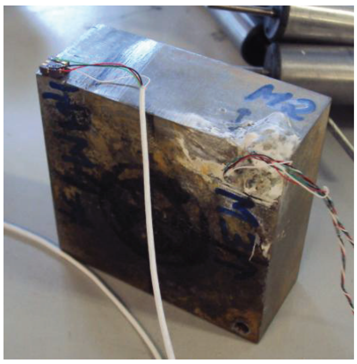

Figure 2.2. Block structure used in the experiment.

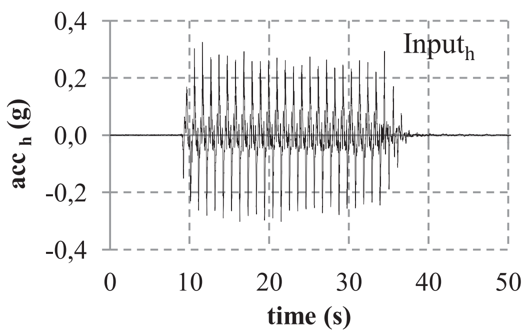

Figure 2.3. Horizontal input motion.

3. EXPERIMENTAL RESULTS AND FINDINGS

The behaviour of the structure-soil system is evaluated through a conveniently designed centrifuge model, where a simple square footing is placed over a saturated deposit of loose sand, as described in section 2, and tested in the centrifuge under simple dynamic loading applied to the model's base in order to induce liquefaction in the sandy deposit. The settlements, accelerations and excess-pore-pressures measured under the footing and in the free-field are described, both during and after the earthquake. It is important to emphasize that the free-field is herein considered as the central line between the 2 structures, which are separated by 13.7 m. This may not totally ensure the existence of a true free-field in that region.

3.1. Settlements

Figure 3.1 shows the settlements of the structure and free-field during and shortly after the earthquake shaking ends. The data shows that, as expected, the settlements measured in the structure are much larger than those experienced by the free-field. On the other hand, Figure 3.2 shows the settlements observed until a new equilibrium condition was reached. Analysing the results depicted in Figure 3.2, it is possible to see that the settlements arising in a significant period of time after the earthquake shaking ends are still highly significant, and so they must be taken into consideration. Moreover, the post-earthquake settlements measured in the free-field and under the structure are not that different – 230mm and 280mm respectively. This means that most of the settlements that are due to the presence of a structure exerting a bearing pressure of 95 *kPa* on the soil take place mostly during the earthquake shaking (Figure 3.1). After that, the settlements observed may result mostly from the dissipation of the excess pore pressure developed during the seismic loading and subsequent soil settlement or, alternatively, the so-called free-field settlements may be affected by the presence of the structures, which tend to increase local settlements.

In Figure 3.2, the dotted line corresponds to a short period of time during which the data acquisition system could not appropriately record the results. Therefore, to make sure that the reconstruction of the earthquake and the post-earthquake data is well conducted, a careful translation of the post-seismic data is performed in order to obtain an acceptable continuity between both results, which is usually fairly simple to verify.

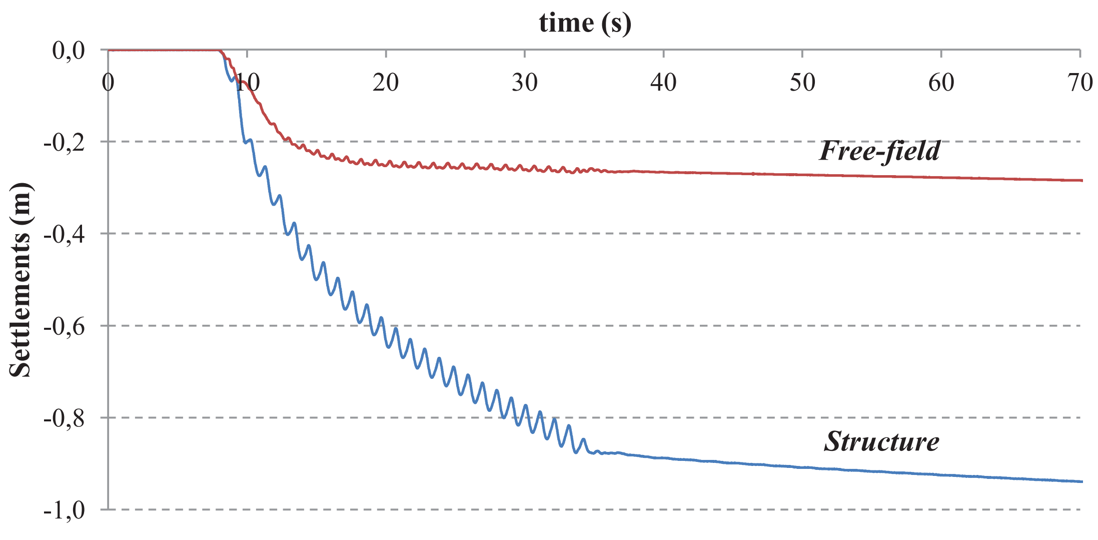

Figure 3.1. Short-term settlement of the structure and free-field – during the earthquake.

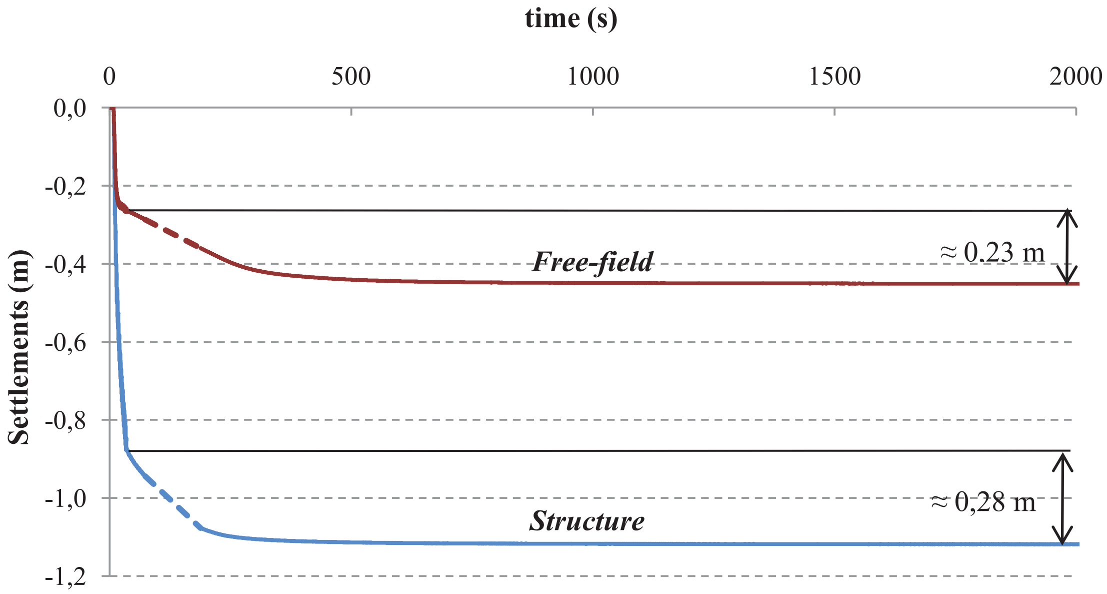

Figure 3.2. Long-term settlement of the structure and free-field – after the earthquake.

3.2. Excess pore pressure generation

Figure 3.3 and 3.4 depict the excess pore pressures (epp) measured during and after the earthquake simulation, respectively, at different positions under the centre of the footing and in the free-field. The corresponding data for the instruments located under the structure show that the initial static shear stress induced by the footing influences the excess pore pressure at different depths during and after the earthquake, this effect being particularly perceptible at shallower depths, as could be logically anticipated.

As the earthquake starts, at all the locations where pore pressure is measured by the transducers, the occurrence of liquefaction is clear, the epp measured starting to increase from the first loading cycle. Figure 3.3 clearly shows that, after that initial increase, the epp tend to stabilize, mainly at deeper levels, the epp values reaching values comparable to the initial vertical effective stress ($r_u \approx 1$). Also, it is possible to see that the rate of increase in epp at deeper levels is more accentuated. On the other hand, in the shallower region closer to the surface, the epp measured tend to increase during the earthquake never reaching steady values. This is expected in the region under the structure, because of the presence of the footing, but this phenomenon was not expected to be measured in the free-field. However, since the free-field is considered to be between the two structures tested (as already stated), it is possible that the results measured in the free-field are somewhat influenced by the presence of structures.

Figure 3.3 clearly shows an interesting phenomenon commonly described as excess pore pressure migration. Immediately after the seismic loading ends, the excess pore pressure variation under the structure is dictated by the hydraulic gradient existing between the structure and the surrounding free-field. In the shallower region, closer to the surface (z = 1m), the excess pore pressure tends to migrate from the free-field to the region under the footing. At other levels, no significant epp variation occurs immediately after the earthquake ends, probably because the instruments are deep enough for the structures to have no influence on the results. At these levels, then, it seems that the epp generation under the footing and in the surrounding soil is negligible.

On the other hand, after this swift post-earthquake epp adjustments mentioned, the resulting epp under the structure tend to dissipate and approach the epp in the free-field at corresponding levels (Figure 3.4), despite never reaching exactly the same value, probably due to some settlement of the instrument placed under the footing. Thus, the epp variation under the structure shortly after the seismic loading event is mostly governed by the epp migration from the free-field. Succeeding dissipation of the epp through time after the earthquake shaking ends progresses in a uniform manner in both levels under the footing and in the free-field.

One final observation that can be seen in the data presented in Figure 3.4 is that it is clear that dissipation initiates at the bottom of the deposit and also that it takes much longer before it starts near the surface. Furthermore, analyzing the results from the levels below to the top, it is possible to see that, as the data correspond to shallower regions, the epp tend to dissipate much slower. This phenomenon is normally observed in this type of tests, where liquefaction occurs, and it is caused by the re-sedimentation of the liquefied sand that starts at the bottom of the container and creates an upward water flow that keeps the sand on the other levels liquefied for a longer period. This is particularly severe for shallow foundations, which can settle for longer periods.

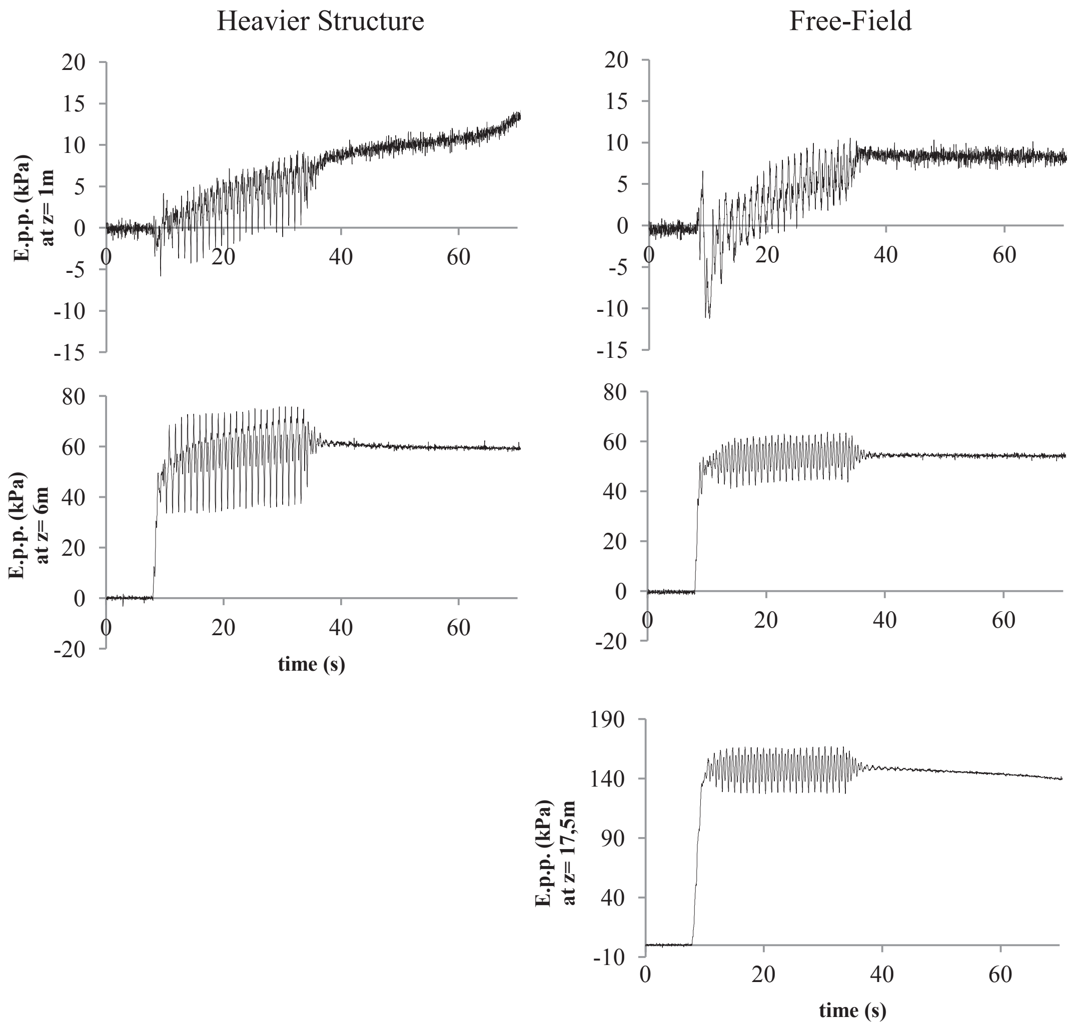

Figure 3.3. Short-term excess pore pressure (epp) at different depths under the footing and in the free-field during the earthquake.

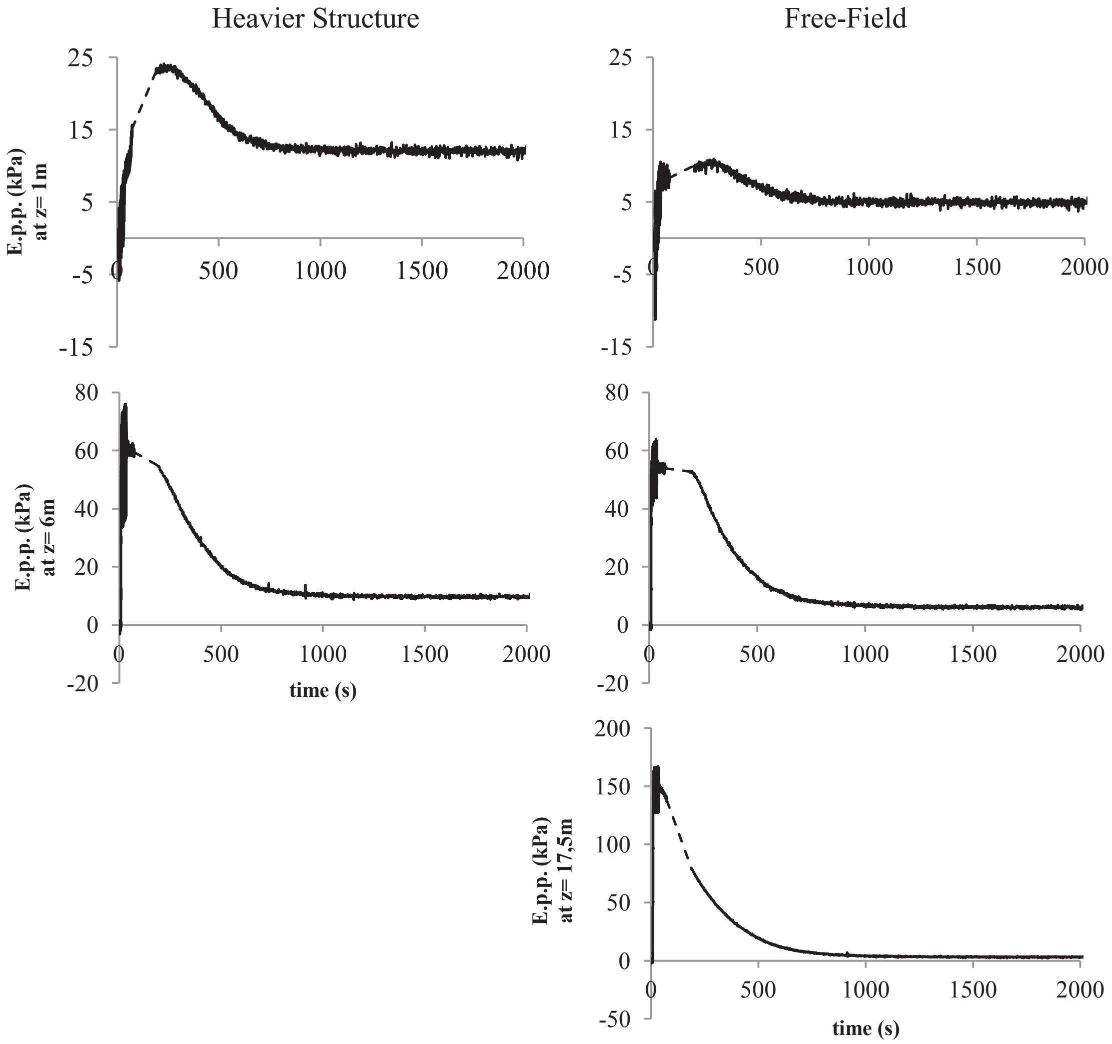

Figure 3.4. Long-term excess pore pressure (epp) at different depths under the footing and in the free-field after the earthquake.

3.3. Vertical motion propagation in the structure

Figure 3.5 presents the time histories of the vertical accelerations measured in the structure and compares these with the vertical input motion. It is important to mention that the designations for left and right sides of the structure are concerned to the cross section view of the centrifuge model layout presented in Figure 2.1.

Figure 3.5 shows that the peak vertical accelerations measured at the structure are much higher than the peak vertical accelerations found in the input motion. Therefore, the vertical accelerations that reach the structure may not be a direct result of the vertical motions imposed by the seismic loading at the base of the model but rather have something to do with the behaviour of the footing or the whole model during the seismic simulation.

On the other hand, Figure 3.5 also shows that the right side of the structure tends to develop higher vertical accelerations then the left side and also that the left and right footing vertical accelerations are in phase. This suggests that the large vertical accelerations observed at the footing are not due to an individual rocking mode of the footing, although it may result from the rocking of the all centrifuge model.

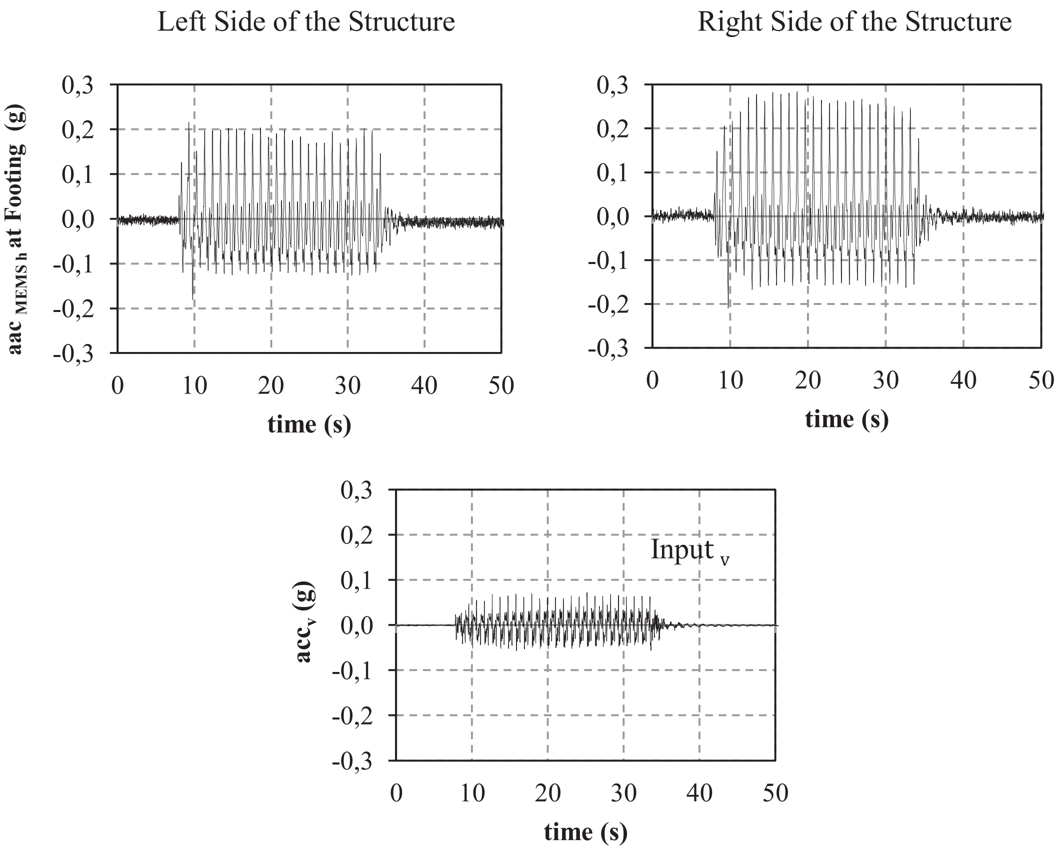

Figure 3.5. Propagation of vertical accelerations in the structures and vertical input motion.

4. CONCLUSIONS

A single centrifuge experiment was made in order to study the performance of a simple square shallow foundation exerting a bearing pressure of 95 *kPa* on the underlying soil, which undergoes the effects of earthquake induced liquefaction as a result selected dynamic loading simulation. The experimental results obtained revealed that:

1. Higher settlements are measured under the structure than in the free-field;

2. The footing and free-field settlements continued for a significant period of time after the end of the seismic loading;

3. The post-earthquake settlements measured in the free-field and structure are not that different, meaning that most of the settlements that are due to the presence of the footing take place mostly during the earthquake motion;

4. The initial static shear stresses induced by the footing influences the excess pore pressure at different depths during and after the earthquake - phenomenon particularly perceptible at shallower depths;

5. Post-earthquake excess pore pressure variation under the footing is dictated by the hydraulic gradient existing between the structure and the free-field – phenomenon known as excess pore pressure migration.

6. The epp measured under the structure tend to dissipate and approach the epp in the free-field at corresponding levels a while after the seismic loading ends, despite never reaching exactly the

same value, probably due to some settlement of the instruments;

7. The epp dissipation through time after the earthquake shaking ends progresses in a uniform manner at each level under the footing and in the free-field;

8. Locations closer to the base tend to dissipate the excess pore pressure faster than at shallower levels, where the epp remains almost constant for some time, proving that the excess pore pressure dissipation in the deposit starts at the bottom and travels from there upwards, as also observed in static liquefaction experiments (Bezuijen & Mastbergen, 1989);

9. Vertical accelerations measured on the structure are much higher than the vertical input motion, the reason for that remaining unclear, but being eventually related to the rocking of the all centrifuge model.

ACKNOWLEDGEMENTS
The authors would like to acknowledge the valuable assistance of the technicians at the Schofield Centre, as well as the financial research scholarship provided by FCT – Fundação para a Ciência e a Tecnologia.

The research leading to these results has received funding from the European Union Seventh Framework Programme (FP7/2007-2013) under grant agreement n° [227887], [SERIES].

REFERENCES

Bezuijen A., Mastbergen D.R. (1989), "Liquefaction of a sand body constructed by means of hydraulic fill". *Proc. 12th. Int. Conf.on soil mechanics and foundation engineering, Rio de Janeiro.*

Madabhushi, S.P.G., Houghton , N.E. and Haigh S.K. (2006). "A new automatic sand pourer for model preparation at university of Cambridge". *In 6th International Conference on Physical Modelling in Geotechnics.*

Madabhushi, S.P.G., Teymur, B., Haigh, S.K. and Brennan, A.J. (2001). "Modelling of Liquefaction and Lateral Spreading". *International Workshop on Earthquake Simulation in Geotechnical Engineering, Cleveland.*

Schofield, A.N. and Zeng, X. (1992). "Design and Performance of an equivalent-shear-beam (ESB) container for earthquake centrifuge modelling". *Tech. Rept. CUED/D-SOILS TR245.Cambridge University, U*K.

Schofield, A.N (1980). "Cambridge geotechnical centrifuge operations". *Geotechnique, 30(3):227–268, 1980.*

Stewart, D. P., Chen, Y. R., and Kutter, B. L. (1998). “Experience with the use of methylcellulose as a viscous pore fluid in centrifuge models”. *ASTM Geotech. Test. J., 21(4), 365–369.*